Accepted Manuscript

Title: Directed precipitation of anhydrous magnesite for improved performance of mineral carbonation of CO_2

Authors: S. Atashin, R.A. Varin, J.Z. Wen

PII: S2213-3437(17)30299-3
DOI: http://dx.doi.org/doi:10.1016/j.jece.2017.06.048
Reference: JECE 1710

To appear in:

Received date: 22-3-2017
Revised date: 19-5-2017
Accepted date: 25-6-2017

Please cite this article as: S.Atashin, R.A.Varin, J.Z.Wen, Directed precipitation of anhydrous magnesite for improved performance of mineral carbonation of CO2, Journal of Environmental Chemical Engineeringhttp://dx.doi.org/10.1016/j.jece.2017.06.048

Directed precipitation of anhydrous magnesite for improved performance of mineral carbonation of CO_2

S. Atashin[a], R. A. Varin[a] and J. Z. Wen[a*]

[a]Department of Mechanical and Mechatronics Engineering, University of Waterloo, 200 University Avenue West, Waterloo, Ontario N2L3G1, Canada

*Corresponding author: john.wen@uwaterloo.ca

Graphic Abstract

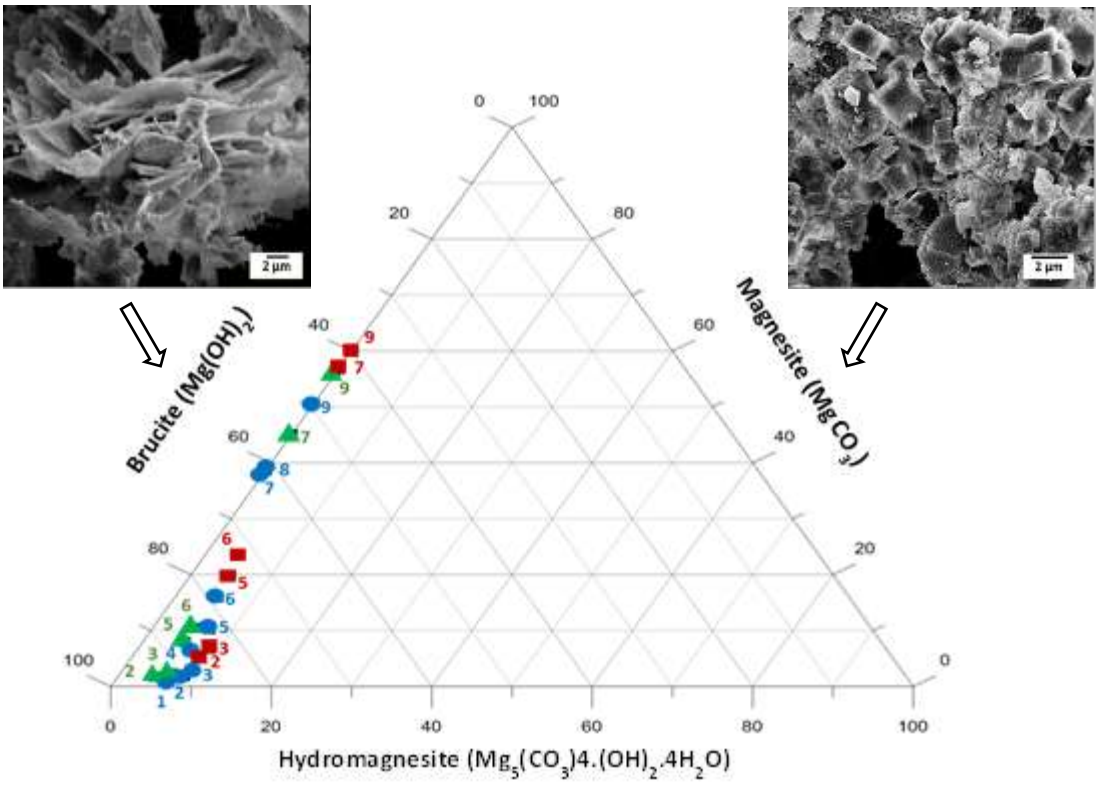

Highlights

- Two separate strategies to control precipitation of anhydrous magnesite have been investigated
- Controlling carbonation process and products through investigating operation parameters such as temperature and pressure
- Enhancement of the heterogeneous precipitation using seeding material

- A ternary phase diagram is achieved which represents the relative concentration of possible precipitated phases: brucite (Mg(OH)2), magnesite (MgCO3) and hydromagnesit (Mg5(CO3)4(OH)2·4H2O)

Abstract

This paper studies the indirect aqueous carbon sequestration via $Mg(OH)_2$ using directed precipitation technique. This technique produces anhydrous $MgCO_3$ (magnesite), the most desirable carbonated phase for sequestration. The formation of magnesite is significantly affected by its kinetics of precipitation in an aqueous carbonation medium. This study considers directed precipitation strategy to control precipitation of anhydrous magnesite through enhancement of the heterogeneous precipitation. Heterogeneous precipitation is implemented using seeding material that could improve the conversion efficiency of the directed carbonation of $Mg(OH)_2$. A ternary phase diagram is achieved which represents the relative concentration of possible precipitated phases: brucite ($Mg(OH)_2$), magnesite and hydromagnesit ($Mg_5(CO_3)_4(OH)_2{\cdot}4H_2O$). The results reveal the fundamental role of heterogeneous precipitation on the magnesite concentration and conversion percentage of $Mg(OH)_2$ wet carbonation process. Two seeding materials, hydrophobic activated carbon and hydrophilic alumina, were tested and the influence of the surface chemistry of varying seeding sites (hydrophobic vs. hydrophilic seeds) was elaborated. At the carbonation temperature of 100°C and 150°C, a heterogeneous precipitation using hydrophilic alumina results in lower concentrations of anhydrous magnesite in precipitated compounds, even as compared to the seedless solution, owing to the hydrophilic properties of alumina. In contrast, use of activated carbon as heterogeneous nucleation sites in an aqueous medium results in a magnesite concentration of around 60% and the corresponding carbonation conversion of about 72% under the controlled condition of 200°C and 30 bar CO_2 pressure.

Keywords: CO_2 sequestration; Mineral carbonation; Aqueous carbonation; Directed anhydrous precipitation.

1. Introduction

Energy production and use cause almost two-thirds of global greenhouse gas (GHG) emission [1-6]. The goal of limiting the global temperature increase to within 2°C by 2100, as set at the 21st Conference of the Parties (COP21) [1], necessities effective strategies for controlling global CO_2 levels. Carbon capture and sequestration (CCS) technologies including mineral carbonation (MC) are considered promising solution that can be implemented immediately while other emission controlling strategies such as renewable energy replacement and energy efficiency improvement are developed [7-14]. Although MC-CCS is thermodynamically favorable, its slow kinetics greatly hinders its use. Various kinetic improvement methods have been suggested to speed up the overall rate of carbon sequestration, such as pre-activation techniques (e.g. mechanical activation, thermal activation and chemical activation). The author's previously explored mechanical pre-activation [15]. However, there is still an urgent need to study the carbonation parameters to enhance the kinetics of carbonation process and achieve favorable carbonated products.

Aqueous indirect carbonation has received significant industrial attention, as it combines the benefits of improved kinetics in aqueous approaches and the process controllability of indirect carbonation [16]. During indirect carbonation route, the overall mineralization process is staged into two major steps; extraction of reactive compounds from original feedstock and later carbonation of extracted compounds. The attraction toward indirect carbonation approach over the direct route is mostly ascribed to its higher efficiency and enhanced overall kinetics of storage. This superiority can be attributed to initial separation of rate controlling silica layers and also, the more efficient control over carbonation parameters [16]. Among the different types of divalent cation bearing feedstock used in mineral carbonation, Mg-bearing materials are the most preferred resources, due to their great abundancy, high theoretical CO_2 storage capacity, and noticeable absorbent element content [9, 17, 18]. $Mg(OH)_2$ is the major reactive compound extracted from such feedstock for indirect carbon sequestration.

Both extraction and carbonation of $Mg(OH)_2$ need to be kinetically improved to facilitate rapid indirect carbon sequestration. The authors studied enhancing the kinetics of extraction stage in their previous research [19] and kinetic enhancement of carbonation stage has been elaborated in current work. Eqs. (1) to (3) summarize the generally accepted elementary steps of the $Mg(OH)_2$ aqueous carbonation process. Eq. (1) shows a dissolution of CO_2 in water (Eq. (1)) which is not permanent and it may go both ways (a double headed arrow). Therefore, a dissolution of $Mg(OH)_2$ material is needed to liberate divalent cations in the solution (Eq. (2)), and finally, the precipitation of carbonated product occurs (Eq. (3)) [9, 15,

20-24]. Precipitation (Eq. (3)) may result in the formation of water as a reaction product, depending upon the type of Mg-carbonate produced. The stoichiometry balance of Eq. (3) also depends upon these products.

$$H_2O + CO_2 \leftrightarrow H^+_{(aq)} + HCO_3^-{}_{(aq)} \leftrightarrow CO_3^{-2}{}_{(aq)} + 2H^+_{(aq)} \quad (1)$$

$$Mg(OH)_{2(s)} + 2H^+_{(aq)} \rightarrow Mg^{+2}_{(aq)} + 2H_2O_{(l)} \quad (2)$$

$$Mg^{+2}_{(aq)} + (HCO_3^-{}_{(aq)} / CO_3^{-2}{}_{(aq)}) \rightarrow \text{Mg-Carbonates} \quad (3)$$

Varying the temperature and pressure results in different hydrous and anhydrous carbonate products during aqueous carbonation of $Mg(OH)_2$ [24, 25]. In the common applicable range of a carbonation process, hydrous carbonates require a higher level of super-saturation (a higher equilibrium constant) than the anhydrous magnesium carbonate ($MgCO_3$-magnesite), suggesting a higher thermodynamic tendency for the formation of anhydrous carbonates vs. hydrous ones. The hydrous precipitates are thermodynamically metastable. In addition, they offer a lower saturation index (SI) of precipitation than anhydrous magnesium carbonates. A saturation index (SI) is the factor which determines solution tendency to form precipitates. This factor compares the actual concentration of solutes under the term of Ion Activation Product (IAP) with thermodynamic solubility product (KSP) to predict the tendency of precipitates formation [26]. However, hydrous carbonate formation can occur more easily due to better kinetics of formation and the formation of the anhydrous magnesite phase is strongly limited by the kinetics of the precipitation process Eq. (3) [25-28].

Anhydrous carbonates are much more favorable compared to hydrous ones owing to their higher storage capability (a lower molecular weight) and thermodynamic stability. So, it is very important to stimulate the kinetics of anhydrous carbonates formation to improve a total carbonation performance. Thus, directing the precipitation toward the formation of anhydrous carbonate phases is desirable, and is referred to as “directed precipitation” in this work. This study aims to promote formation of anhydrous magnesite for the final goal of more efficient $Mg(OH)_2$ carbonation process with the more stable carbonated products. Since the formation of favorable magnesite compound is mainly limited by the kinetics of formation, heterogeneous precipitation strategy is proposed to improve the efficiency of directed precipitation by enhancing the kinetics of magnesite formation.

A number of researchers have investigated the kinetics and mechanism of magnesite ($MgCO_3$) precipitation during aqueous carbonation of $Mg(OH)_2$. Their main focus has been on predicting most likely carbonate precipitates to be formed as a function of applied conditions such as temperature and pressure

[29-33]. The enhancement of precipitation kinetics was studied in [24, 34-36]. For example, the effect of heterogeneous nucleation on precipitation of calcium carbonate in an aqueous solution was studied by Chevalier [35] considering two different hydrophobic and hydrophilic nucleation sites. However that research is aimed to inhibit the formation of calcium carbonates in heat exchangers and the possible effect of heterogeneous precipitation on the improvement of carbonation process, under applicable carbonation conditions is not the focus. Similarly, Swanson et al. [24] studied the effect of heterogeneous precipitation on the aqueous carbonation of $Mg(OH)_2$ using magnesite and alumina seeds with the goal of directed carbonation. Their results show that the magnesium carbonate seeds are more prone to form favorable magnesium carbonate precipitates as compared to the alumina seeds. This effect was mainly attributed to similarity between the crystal orientation of magnesium carbonate seeds and magnesite precipitates. The possible effect of surface wettability was not evaluated [24].

Considering the previously proven effect of heterogeneous seeding on the formation of precipitates, this study aimed to improve the process of directed carbonation of $Mg(OH)_2$ using heterogeneous precipitation sites. The effect of wettability parameter was evaluated, addressing the current gap in the effect of surface wettability of heterogeneous nucleation sites (seeds) on directed carbonation. This effect was considered through the comparison of the effects of hydrophobic and hydrophilic seeds on carbonation efficiency and magnesite concentration.

The first phase of this study thoroughly explored the quantitative effects of temperature and pressure on magnesite content and carbonation conversion percentage, in order to understand the path of directed carbonation of $Mg(OH)_2$ toward favorable anhydrous carbonates. In this phase, the correlation between the concentration of magnesite and overall carbonation conversion was assessed. The results of first phase was used as a baseline to clarify the effect of heterogeneous precipitation strategy, investigated in the second phase. In the second phase, a heterogeneous precipitation through seeding to enhance the rate of magnesite formation, was studied. Two different seeding materials with varying wettability properties were used with the objective of enhancing the kinetics of precipitation using the general effect of heterogeneous nucleation sites. The possible effects of different precipitation sites with varying wettability properties on the water content of precipitated carbonates were examined. The main objectives of this study are, to quantitative evaluation of the effect of carbonation temperature and pressure on the directed precipitation of $MgCO_3$ during the aqueous carbonation of $Mg(OH)_2$, by investigating the variation in the magnesite concentration and the total extent of carbonation conversion; to assess the general effect of heterogeneous nucleation on the kinetics enhancement of the anhydrous magnesite formation, under varying temperature and pressure conditions; and to investigate the

influence of dissimilar surface properties of heterogeneous nucleation sites on directed precipitation, under different temperature and pressure conditions, during aqueous carbonation. A ternary phase diagram, which represents the relative concentration of possible precipitated phases: brucite ($Mg(OH)_2$), magnesite and hydromagnesit ($Mg_5(CO_3)_4(OH)_2{\cdot}4H_2O$) under different carbonation conditions, is to be plotted.

2. Experimental methods

Magnesium hydroxide ($Mg(OH)_2$) powders (Alfa Aesar 1039-42-8; 95-100% assay) were used in this research as a Mg-bearing source during aqueous carbonation. In each carbonation test, 3 g of $Mg(OH)_2$ was added to 100 cc distilled water (a concentration of around 0.5 molar).

Carbonation reactions were performed in a 4650 Parr high-temperature, high-pressure reaction vessel. The vessel was evacuated and purged with CO_2 gas prior to setting the desired carbonation pressure and temperature. In all cases, the reactor was heated from room temperature to the desired carbonation temperature, at a rate of about 10 deg.min^{-1}, and then was kept under adjusted constant temperature for 60 min. In all cases the carbonation pressure was adjusted to the desired value through opening the valve connected to inlet CO_2 bottle. Fig. 1 shows a schematic of the carbonation setup. A combination of reaction temperatures and pressures was selected based on the saturated water thermodynamic table [37], such as to ensure that the solvent water would not evaporate under applied conditions and the gas phase remained pure CO_2. Carbonation temperatures of 100, 150 and 200°C and CO_2 pressure of 10, 20, 25 and 30 bar were tested.

The experimental occur under either seedless or seeding conditions. The alpha alumina (Al_2O_3) particles (Alfa Aesar 1344-21-1; 99.9% assay; <1.0 µm APS; 2-4 m^2/g SSA) were used as hydrophilic seeding materials. Activated carbon powders (MTI TF-B-520; 5 µm APS; 2000 m^2/g SSA) were applied as hydrophobic seeding sources. To supply an equal surface area of heterogeneous nucleation sites during carbonation, 1.0 g of alumina or 1.5 mg of activated carbon powders was added to the carbonation solution.

After carbonation process, the reactor was cooled to room temperature, and the carbonation solution, including the carbonated precipitates, was filtered using 2.5 µm pore size filtering papers (Whatman 1442-055; grade 42). To evaporate adsorbed moisture from the powders, the recovered precipitates were oven dried for two hours at 200°C, after filtration.

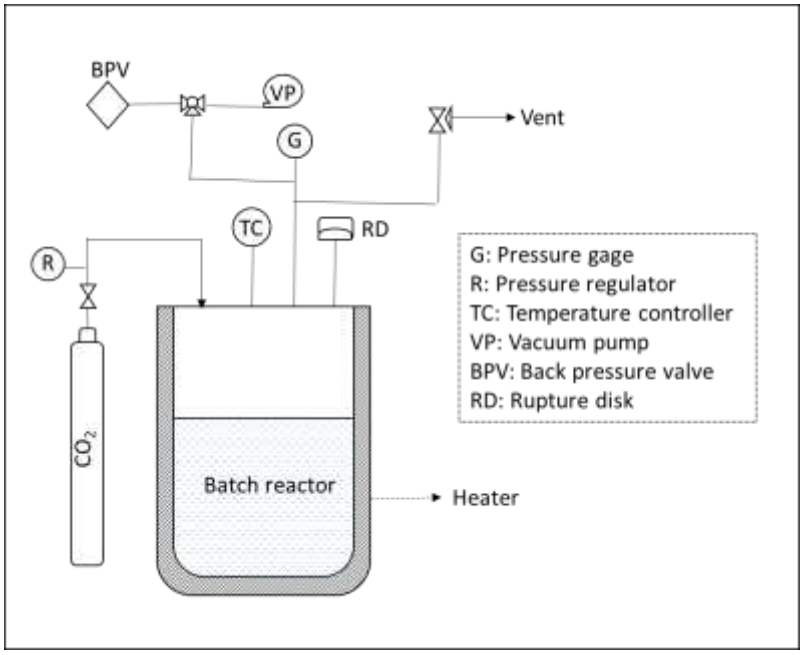

Fig 1. Schematic overview of $Mg(OH)_2$ aqueous carbonation apparatus (The drawing is not on scale).

The dried, filtered solid products were the aggregates in the size range of 15 to 50 µm. Thermal analyses were performed on solid products in a combined DSC/TGA thermal analyzer device (NETZSCH STA 449F3A-0918-M Jupiter), under argon atmosphere with the flow rate of 20 mL/min. An alumina crucible was used as a sample container. In all cases, the mass of solid sample was 10±1 mg and specimens were heated from room temperature to 750 °C at a rate of 10 deg.min-1. SEM micrographs were obtained via the secondary electron detector of LEO 1550 Zeiss SEM at 10 kV. To promote the conductivity of samples for SEM imaging, samples were gold coated prior to SEM analysis using a1 UHV spotter system for 139 seconds, with a current of 20 mA. XRD phase analysis was performed using an INEL XRG 3000 Powder Diffractometer, via monochromic Cu Kα1 radiation with the wavelength of 0.15406 nm, generated by the accelerating voltage and current of 30 kV and 30 mA, respectively.

3. Results and discussion

3.1. Effects of temperature and pressure on directed magnesite precipitation in seedless aqueous carbonation of $Mg(OH)_2$

The effects of temperature and pressure on the efficiency of magnesite formation, as a potential favorable anhydrous carbonation product during $Mg(OH)_2$ carbonation, were characterized. This initial research phase was designed to examine the effect of applied carbonation parameters (temperature and pressure) on the efficiency and magnesite concentration during seedless $Mg(OH)_2$ carbonation process. This phase is also aimed to evaluate the role of magnesite concentration on the overall carbonation efficiency. The results of this research phase, were used as a baseline to clarify the effect of heterogeneous precipitation strategy, applied in a later phase.

Seedless $Mg(OH)_2$ aqueous carbonation was evaluated at temperatures of 100, 150 and 200°C. Pressure was adjusted to 10, 20, 25 and 30 bar. The carbonation products were then filtered, dried and analyzed to track the presence and relative concentration of brucite ($Mg(OH)_2$), hydromagnesite ($Mg_5(CO_3)_4(OH)_2{\cdot}4H_2O$) and magnesite ($Mg(CO_3)$). These phases are the typical products of aqueous carbonation of $Mg(OH)_2$ in the applied range of temperatures and pressures in this research, in accordance with the available literature data that were evaluated from a standpoint of the thermodynamic stability of possible carbonated precipitates [24, 25, 28, 30, 33]. Fig. 2 presents the SEM micrograph of carbonated products (magnesite and hydromagnesite), showing the rhombohedral structure of magnesite (Fig. 2a) vs. the sheet like morphology of hydromagnesite (Fig. 2b).

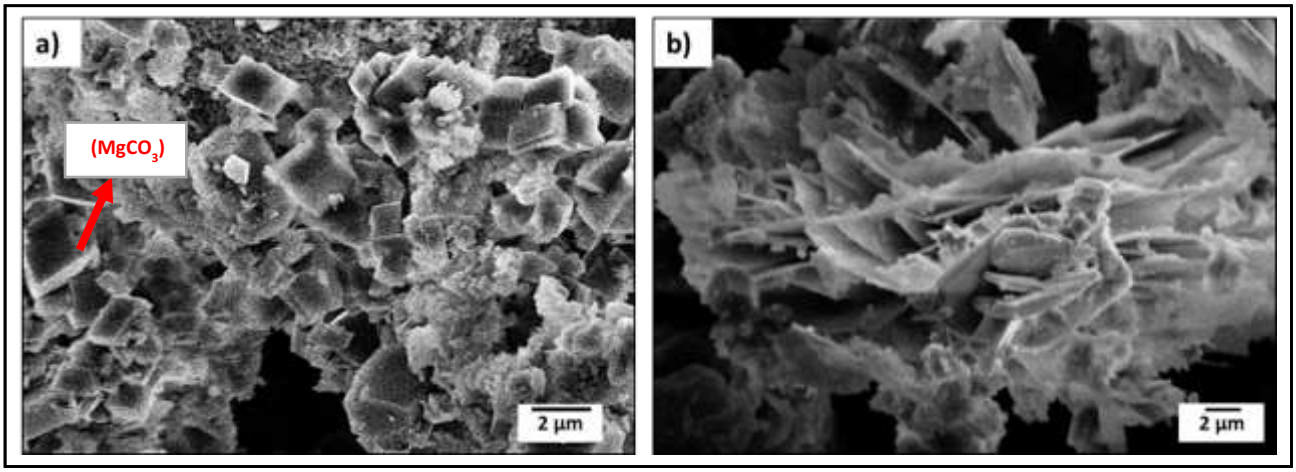

Fig 2. SEM micrograph of hydrous and anhydrous precipitated carbonate compounds in $Mg(OH)_2$ aqueous carbonation process. a) Magnesite ($MgCO_3$) formed at 200°C and 20 bars, b) hydromagnesite ($(Mg_5(CO_3)_4(OH)_2{\cdot}4H_2O)$) formed at 150°C and 20 bars.

In the initial stage, carbonation products were analyzed using XRD method for qualitative evaluation of possibly formed crystalline carbonation precipitates. Fig. 3 shows the XRD patterns of precipitated phases,

at the varying applied temperature and pressure conditions. Comparing the XRD patterns illustrated in Fig. (3-a), it seems that temperature exerts a significant effect in a direct precipitation of $Mg(OH)_2$, so that no obvious diffraction peak of hydrous magnesites is observed at the carbonation cases at 200°C, and favorable anhydrous magnesite was shown to be the sole crystalline carbonated product during aqueous carbonation of $Mg(OH)_2$ under 200°C. It needs to be mentioned that just the XRD peaks of magnesite, hydromagnesite and brucite are labeled in this figure and the possible peaks of alumina that might have overlapped with the diagnosed peaks of considered compounds are not shown.

Knowing that an XRD method is not capable of detecting the possibly amorphous phases during carbonation, thermal analysis was performed as a complimentary technique to evaluate both crystalline and amorphous phases. Also, a quantitative investigation of the percent fraction of possible carbonation products was carried on through thermal decomposition of dried carbonated products in a thermogravimetric (TG) apparatus under an inert argon atmosphere.

Fig. 4 presents the thermogravimetric analysis (TGA) results attributed to the decomposition of different carbonated products at a temperature range from room temperature to 750°C. Different chemical compounds are characterized by a varying temperature range of decomposition related to the specific type of chemical bonding in their structure. Hence, the mass fraction of each carbonated product (brucite, magnesite and hydromagnesite) can be calculated based on the TGA mass percentage variations at a specific temperature range, attributed to the decomposition of that particular compound. Eq. (4) presents the decomposition (dehydroxylation) reaction of brucite which was reported to take place at the range of around 400-450°C [24, 38, 39].

$$Mg(OH)_{2(s)} \rightarrow MgO_{(s)} + H_2O_{(g)} (\sim 400\text{-}450^{\circ}C) \quad (4)$$

Hollingbery [39] performed a comprehensive study of a decomposition mechanism of hydromagnesite through reviewing and evaluating the previously-suggested mechanisms and theories [39-44] and presented a three stage dissociation mechanism during the thermal decomposition of hydromagnesite.

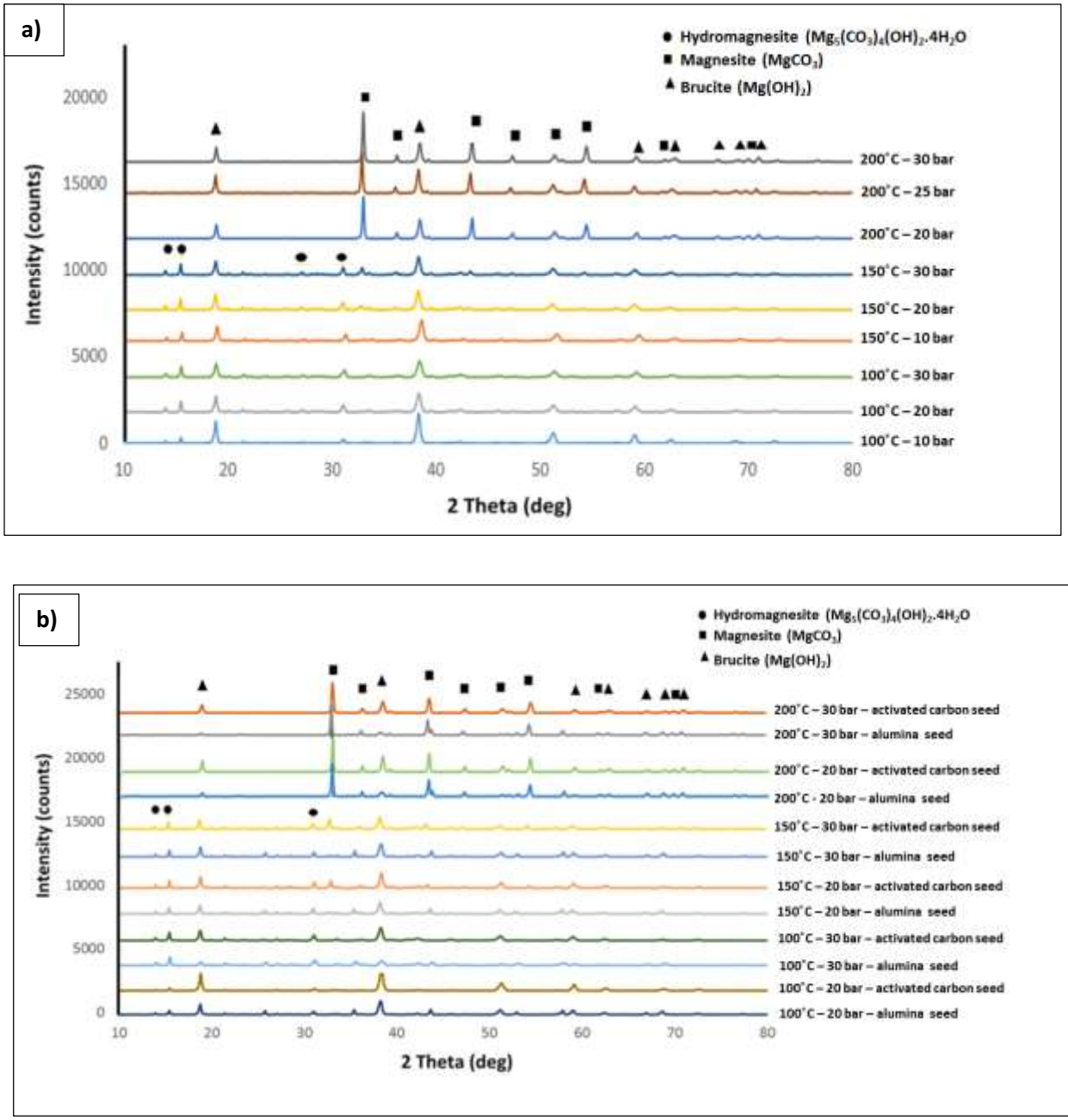

Fig 3. XRD patterns of precipitated phases, formed during aqueous $Mg(OH)_2$ aqueous carbonation. a) seedless carbonation. b) carbonation with seeding sites (alumina and activated carbon).

Based on the proposed mechanism, hydromagnesite decomposes through three separate stages of dehydration (release of structural water) Eq. (5), dehydroxylation (repealing the hydroxyl group) Eq. (6), and the final decarbonation stage Eq. (7) [24, 31, 33, 38].

$$Mg_5(CO_3)_4(OH)_2 \cdot 4H_2O_{(s)} \rightarrow Mg_5(CO_3)_4(OH)_{2(s)} + 4H_2O_{(g)} \quad (\sim 220\text{-}350^{\circ}C) \tag{5}$$

$$Mg_5(CO_3)_4(OH)_{2(s)} \rightarrow (Mg)_4(CO_3)_{4(s)} + MgO_{(s)} + H_2O_{(g)} \quad (\sim 350\text{-}460\ ^{\circ}C) \tag{6}$$

$$(Mg)_4(CO_3)_{4(s)} \rightarrow 4MgO_{(s)} + 4CO_{2\ (g)} \quad (>515^{\circ}C) \tag{7}$$

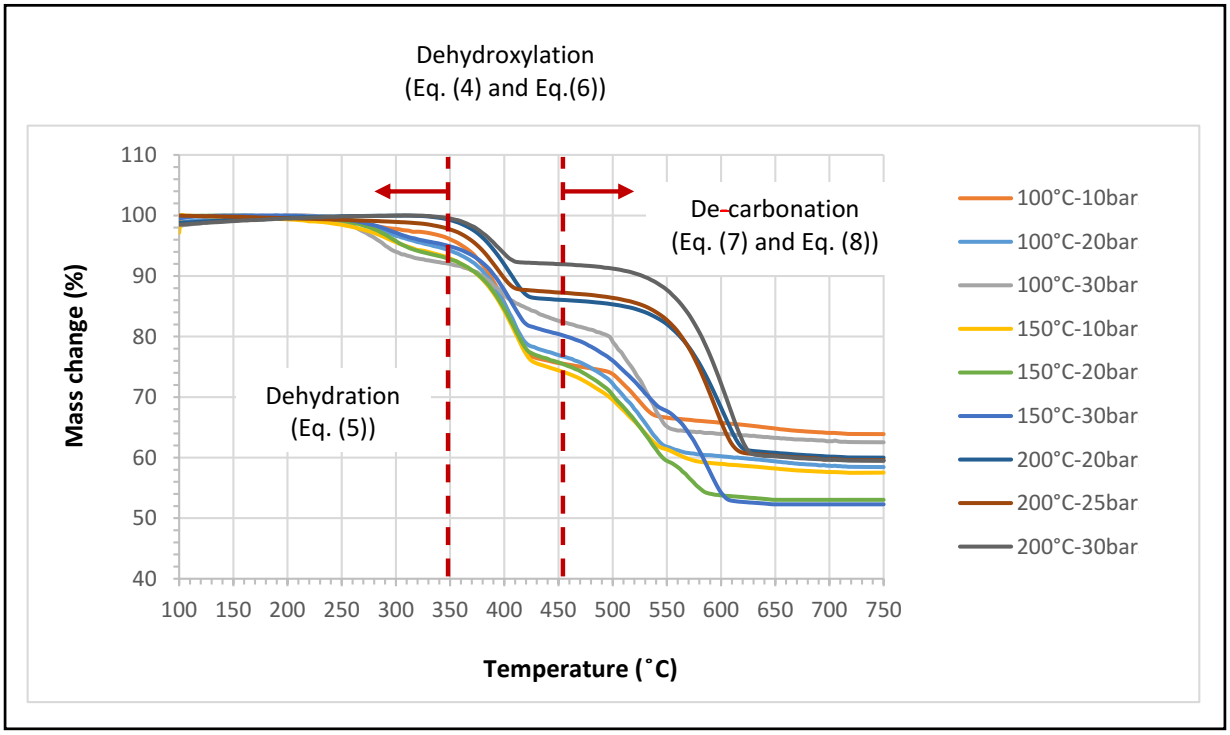

Fig 4. TGA thermal decomposition graph of precipitated phases, formed during aqueous carbonation of $Mg(OH)_2$.

Subsequently magnesite, as the most favorable product of $Mg(OH)_2$ aqueous carbonation, decomposes at the temperature higher than 460˚C based on Eq. (8).

$$MgCO_{3(s)} \rightarrow MgO_{(s)} + CO_{2\ (g)} \quad (>460^{\circ}C) \tag{8}$$

Considering the decomposition reactions and corresponding temperature ranges, TGA curves were sectioned into three separate ranges in Fig. 4, representing the first section of hydromagnesite dehydration in the approximate range of 220-350˚C, the second section of hydromagnesite and brucite dehydroxylation in the approximate range of 350- 460˚C, and the third section of hydromagnesite and

magnesite decarbonation over 460°C. Since there is a clear overlap between the dehydroxylation of brucite (Eq. (4)) and hydromagnesite (Eq. (6)), as well as decarbonation of magnesite (Eq. (8)) and hydromagnesite (Eq. (7)), the isolated dehydration temperature range of hydromagnesite (220-350°C) has been considered as a separate stage in estimating the mass percentage of hydromagnesite (Eq. (5)).
The mass percentage of hydromagnesite can be calculated using Eq. (9), based on the stoichiometry of the hydromagnesite dehydration reaction (Eq. (5)).

$$\text{Hydromagnesite (mol \%)} = \frac{\text{TGA mass change (\%) in the range of hydromagnesite dehydration } (\sim 220\text{-}350^{\circ}\text{C})}{\text{molar number of water}(4) \times \text{molar mass of water } (18\ \text{g.mol}^{-1})} \quad (9)$$

Although in a similar study by Swanson et al. [24], a thermal decomposition range of over 460°C has been specifically addressed to magnesite decarbonation, the present authors believe that considering the previously suggested mechanisms and dissociation models of hydromagnesite [24, 31, 33, 38], there would be a strong overlap between the decarbonation range of magnesite and hydromagnesite. Hence, this temperature range would not result in a concentration of pure magnesite and the initial dehydration range of hydromagnesite has been addressed as a unique decomposition range when calculating the hydromagnesite concentration in a magnesite- brucite- hydromagnesite mixture as given by Eq. (9). Since the decarbonation of both magnesite (Eq. (8)) and hydromagnesite (Eq. (7)) is possible at the thermal range of over 460°C (at the third stage, shown in Fig. (4)), the corresponding mass reduction owing to a decomposition at this temperature range has been attributed to the combined decarbonation of magnesite and hydromagnesite compounds. The pure concentration of magnesite can then be estimated upon deduction of the hydromagnesite portion which can be calculated based on Eq. (9). Subsequently, considering the stoichiometry of hydromagnesite decomposition reactions (Eq. (5) to Eq. (7)), the contribution of mass reduction as a result of hydromagnesite decarbonation can be calculated and deduced in the thermal range of over 460°C, to estimate the net concentration of the magnesite phase (Eq. (10)). Hydromagnesite mol % was calculated using Eq. (9). Obviously, the balanced value over 100 presents the molar percentage of brucite in the analyzed compound.

$$\text{Magnesite (mol \%)} = \frac{\text{TGA mass change (\%) in the thermal range of over } 460^{\circ}\text{C}}{\text{molar mass of } CO_{2(g)}\ (44\ \text{g.mol}^{-1})} - (\text{hydromagnesite (mol \\%)} \times 4) \quad (10)$$

It needs to be mentioned here that the ranges of mass change variation in TGA graphs were set and justified based on the corresponding TGA first derivative curve (dTGA) for an accurate mass change period selection in each section.

A ternary phase diagram presented in Fig. 5 is plotted based on the relative molar percentage of each component, under different applied conditions. As shown in Fig. 5, no hydromagnesite phase forms under 200˚C, and anhydrous magnesite is the only carbonated product formed at the highest temperature of 200˚C. This result was also confirmed by the XRD diffraction patterns (Fig. 3-a) which shows no evidence of crystalline hydromagnesite diffraction peaks for 200˚C carbonation cases.

Also, as shown in Fig. 5, the molar percentage of the magnesite compound, as the intended carbonated phase in the directed carbonation of $Mg(OH)_2$, increases as a function of both temperature and pressure. As shown in Fig. 6, the magnesite molar percentage (M%), which was analyzed based on the thermal decomposition in TGA curves as explained earlier, increases as a function of both temperature and pressure. However, the effect of temperature increase on the increment of M% is more profound than that of the pressure.

To further clarify the effect of temperature and pressure on the magnesite percentage value, the mechanism of carbonate precipitate formation during the $Mg(OH)_2$ carbonation process must be taken into consideration. The mechanisms of the formation of magnesite in aqueous carbonation solutions have been addressed and evaluated in the literature [24, 25, 28, 34, 35]. According to the suggested mechanism, magnesite mainly precipitates through the transformation of pre-formed hydrous carbonates such as hydromagnesite [24, 25, 27-30, 45]. The transition stage of intermediate hydromagnesite to magnesite transformation was considered as a bottle neck stage in the magnesite precipitation process.

At high temperatures, the liberation of water molecules from hydromagnesite structure is facilitated, the transition of pre-formed hydromagnesite to magnesite is enhanced and magnesite precipitation is enhanced [34]. This mechanism could reasonably explain why during a certain precipitation period (60 min), the extent of precipitated magnesite increases as a function of temperature. Therefore, no trace of hydromagnesite has been recorded in either XRD (Fig. 3-a) or TGA (Fig. 6).

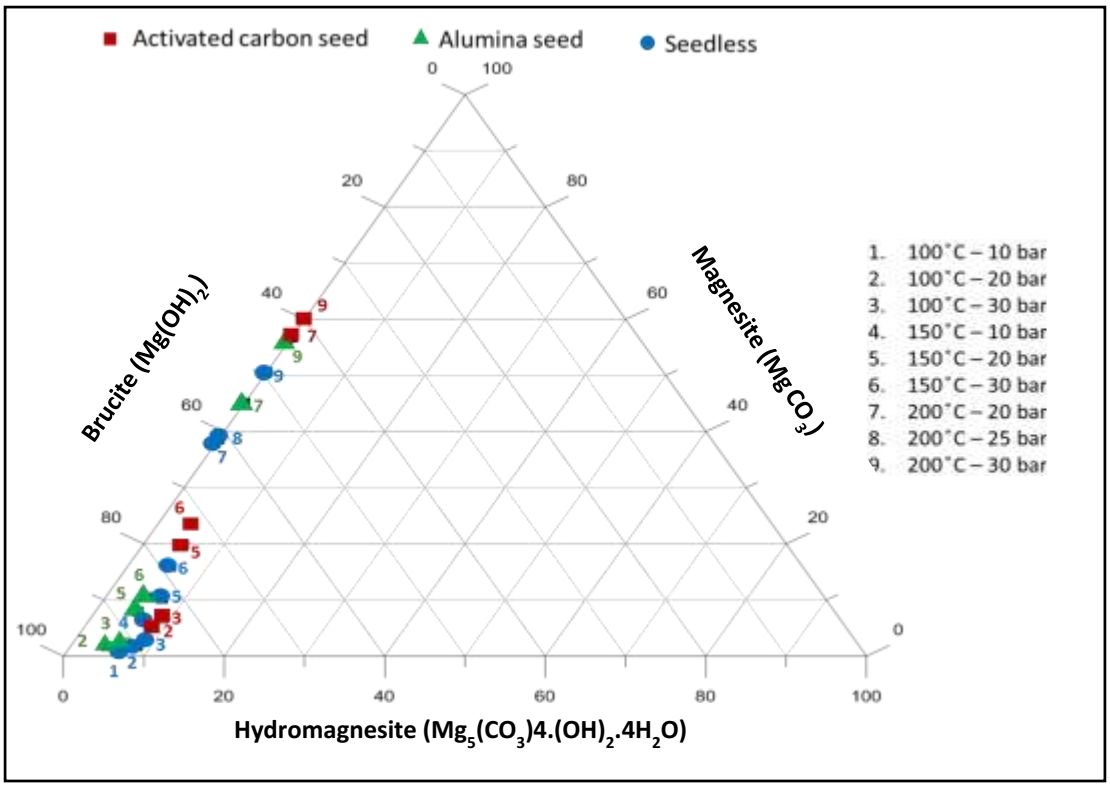

Fig 5. Phase diagram, representing the relative concentration of brucite ($Mg(OH)_2$), magnesite ($MgCO_3$) and hydromagnesite ($Mg_5(CO_3)_4.(OH)_2.4H_2O$) in the precipitated phases, formed during aqueous carbonation of $Mg(OH)_2$.

In regard with the reported zero concentration of hydromagnesite at 200˚C, it needs to be emphasized that, although XRD method is solely capable of crystalline phase detection, the possibility of the presence of amorphous hydromagnesite phase is negligible, considering the outcome of thermogravimetric analysis which is capable of detecting both amorphous and crystalline phases. The extent of magnesite precipitation also increases as a function of pressure as is also recorded in previous studies [25, 29, 33]. However, as shown in Fig. 6, the effect of pressure on increasing the magnesite content is more noticeable at higher temperatures. This observation may be attributed to the fact that the rate of dissolution of CO_2 gas in the aqueous solution as a first stage of $Mg(OH)_2$ carbonation (Eq. (1)), decreases with a temperature increase. Hence, at high temperatures, a CO_2 pressure increase can have a greater effect through promoting CO_2 concentration in the solution.

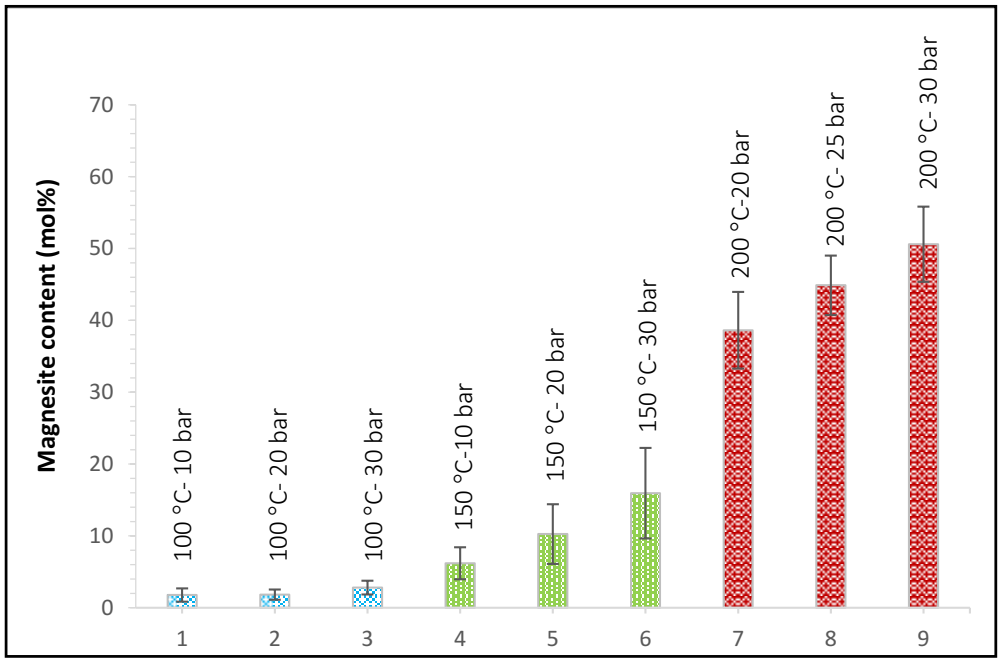

Fig 6. Magnesite molar concentration variation as a function of carbonation temperature and pressure, in precipitates formed during seedless aqueous carbonation of $Mg(OH)_2$.

In the next stage, the effect of temperature and pressure parameters on the total value of conversion percentage was studied. The carbonation conversion percentage is defined as the amount of CO_2 which is stored in the material relative to the maximum theoretical capacity of a considered material to store CO_2 [9, 46]. In order to calculate the extent of conversion percentage under each condition, the mass ratio of actual CO_2 released during TGA thermal decomposition to the maximum theoretically possible CO_2 release was calculated. The maximum theoretically possible CO_2 release was considered as the amount of CO_2 gas that could be released during TGA thermal decomposition, if the total product of $Mg(OH)_2$ carbonation is anhydrous magnesite. Magnesite was chosen as a reference material, with the maximum possible CO_2 release in thermal decomposition, having the highest Mg to C ratio and lowest molecular weight. It results in the highest density of CO_2 storage, among all the other possible products of carbonation in proposed $Mg(OH)_2$ carbonation [46]. With this definition, the total amount of carbonation conversion percentage can be calculated from Eq. (11).

$$\text{Carbonation conversion (\%)} = \frac{(\text{Hydromagnesite mol\%}\times 4)+(\text{Magnesite mol\%})}{100} \qquad (11)$$

Fig. 7 shows the trend of $Mg(OH)_2$ carbonation conversion percentage as a function of temperature and pressure. The trend of conversion percentage variation as a function of temperature and pressure is very close to that presented for the molar percentage of magnesite in Fig. 6. The similarity between Fig. 7 and Fig. 6 points out towards the important role of the directed precipitation of anhydrous magnesite on improving carbonation efficiency. Adding the great thermodynamic stability of magnesite to the scenario, the importance of directed precipitation is even more significant.

3.2. Effect of heterogeneous seeding on directed precipitation of anhydrous magnesite under varied temperature and pressure conditions during aqueous carbonation of $Mg(OH)_2$

Because the kinetics of magnesite formation is the most important barrier to the directed precipitation of $MgCO_3$ [24], heterogeneous nucleation was proposed and implemented in this phase of research. As is well-known from the theory of precipitation processes, heterogeneous nucleation is capable of enhancing the total kinetics of precipitation, through reducing the activation energy barrier of nucleation [24, 35, 36, 47-50]. This reduction has been proven and explained through considering the geometry of nuclei and the changes in the acting interfacial surfaces. Heterogeneous nucleation can successfully add a negative energy contribution term (as a result of the destruction of the seed to liquid interface), to the general terms of free energy variation during nucleation process and enhance the kinetics of nucleation stage [47-49].

Knowing that heterogeneous seeding is fairly capable of enhancing the rate of precipitation in $Mg(OH)_2$ aqueous carbonation, seeding sites were added to the solution with the goal of possible enhancement of directed precipitation. The effect of dissimilar heterogeneous sites on kinetics of magnesium carbonate ($MgCO_3$) formation was evaluated. Alumina (Al_2O_3) and activated carbon seeds were examined as hydrophilic and hydrophobic precipitation sites, respectively. The total surface area of these seeding materials was kept constant in order to eliminate the effect of precipitation site availability. The effect of different seeds' surface properties on the carbonation conversion percentage and magnesite content was evaluated under varying temperature and pressure conditions to track the performance of seeding sites as a function of carbonation conditions.

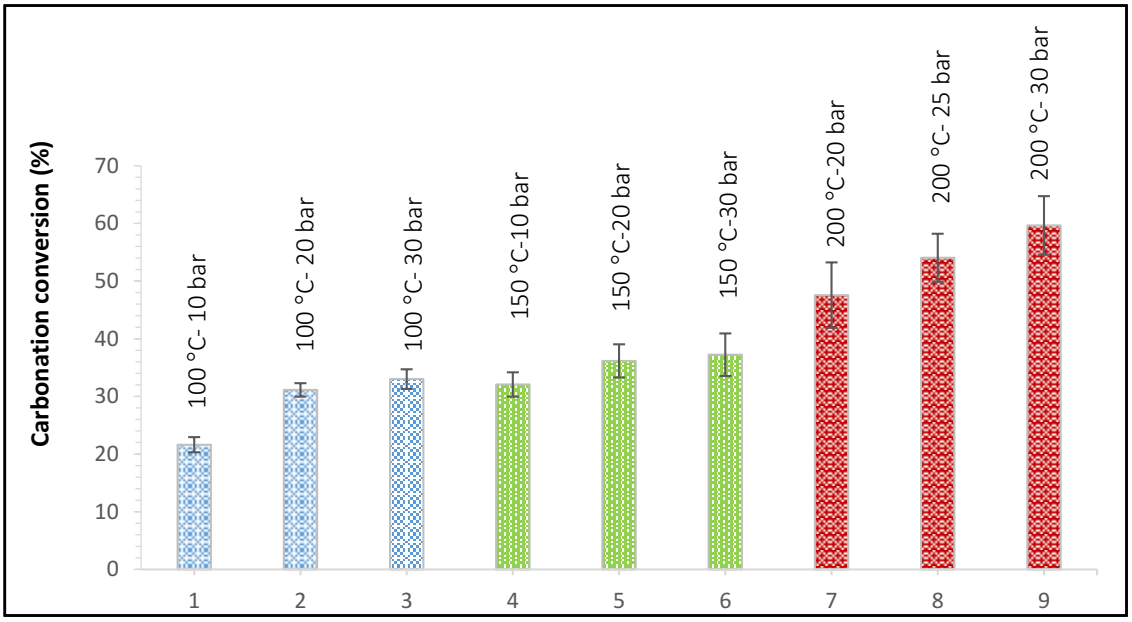

Fig 7. Carbonation conversion percentage variation as a function of carbonation temperature and pressure in precipitates formed during seedless aqueous carbonation of $Mg(OH)_2$.

Aqueous carbonation of $Mg(OH)_2$ was performed at temperatures of 100, 150 and 200°C under the CO_2 pressures of 20 and 30 bar. At each condition, seedless and heterogeneous precipitation was tested and compared.

In the first stage, crystalline carbonated products were analyzed using XRD method. The results are included in Fig. 3-b. Similar to the previous research stage explained in section (3.1), the brucite ($Mg(OH)_2$), hydromagnesite ($Mg_5(CO_3)_4(OH)_2{\cdot}4H_2O$) and magnesite ($Mg(CO_3)$) phases were identified in diffraction patterns to evaluate the qualitative effect of the preferred nucleation process on the type of precipitated phases. Based on the XRD results in Fig. 3-b, the crystalline hydromagnesite phase was not found at high temperature condition (200°C). Again, TGA was performed as a complement to XRD analysis, to compensate for the weakness of XRD method in analyzing the possible amorphous carbonation products. Fig. 8 shows the TGA thermal decomposition plots of the carbonation products which were utilized to calculate the total conversion percentage of carbonation process, as well as the molar concentration of the possible hydromagnesite, magnesite and brucite phases, based on the method explained in section (3.1). The ternary diagram presented in Fig. 5 includes the data corresponding to heterogeneous carbonation as well as those recorded under seedless condition. Similar to the results of seedless precipitation, the effect of temperature increase on directing the $Mg(OH)_2$ carbonation process through the formation of anhydrous magnesium carbonate (magnesite) is clearly shown. The molar percentage of

magnesite increases with increasing temperature. Thus, hydromagnesite content is not significant at the high temperature of 200 ˚C, neither as an amorphous phase monitored with TGA (Fig. 5), nor as a crystalline phase detected by XRD (Fig. 3-b). The noticeable effect of temperature on the formation of $MgCO_3$ can be explained based on the previously discussed mechanism of magnesite formation, from the intermediate hydromagnesite phase, since high temperature speeds up the rate of hydromagnesite to magnesite transition through facilitating the liberation of water molecules [34].

Comparing the data points attributed to the activated carbon and alumina seeds in the ternary carbonation diagram presented in Fig. 5, under similar temperature and pressure conditions, the magnesite molar concentration is higher for activated carbon. Fig. 9 shows that the magnesite concentration increases as a function of temperature and pressure in both seeding conditions, owing to the enhanced kinetics of hydromagnesite to magnesite transition or promoting the dissolution of CO_2 in aqueous solution as a first stage of carbonation (Eq. (1)). The trend in Fig. 9 shows that the concentration of anhydrous magnesite phase is higher using activated carbon carbonation, compared to both alumina and seedless carbonations under similar applied temperature and pressure conditions.

This result may be attributed, firstly, to the role of activated carbon as a heterogeneous site of nucleation, which decreases the energy barrier to nucleation [47-49]. On the other hand, unlike the alumina seed, activated carbon shows a water repelling effect, known as hydrophobic property, and so tends to repel water molecules. Because of this intrinsic hydrophobic property of activated carbon, the kinetics of the water-repellent process during hydromagnesite to magnesite transition can be enhanced, resulting in a higher concentration of magnesite precipitation, compared to hydrophilic alumina seeds. The effect of wetting properties of seeding materials on the propensity of nucleation and adsorption of precipitates was also investigated by Chevalier [35] in an study on the effect of surface wetting properties on the nucleation and adhesion of calcium carbonate ($CaCO_3$) in aqueous solution. Different hydrophobic and hydrophilic nucleation sites were evaluated in his research. The results of his study demonstrated that when the nucleation site did not promote any specific orientation of precipitates crystal, hydrophilicity showed a negative effect on nucleation of calcium carbonate precipitates. The logic behind the effect of surface wetting properties on precipitation formation was explained through analysis of surface free energies, involved in the nucleation stage. Referring to [35] the net surface free energy of a crystal nuclei on nucleation site is a function of interfacial free energy of precipitate/solution ($\Upsilon_{p/sol}$) and nucleation site/solution ($\Upsilon_{ns/sol}$) interfaces. In the case of hydrophilic nucleation sites, the formation of nucleation site/solution bond is favored over the formation of precipitate/solution bonds and the nucleation site shows higher tendency to form OH-bond with the solution water molecules rather than carbonate ions.

This hydrophilic property ends up with the noticeable reduction in $\Upsilon_{ns/sol}$ as compared to $\Upsilon_{p/sol}$. Hence, the net surface energy of formation of carbonated precipitates nuclei increases and causes a reduction in nucleation density vs hydrophilicity [35].

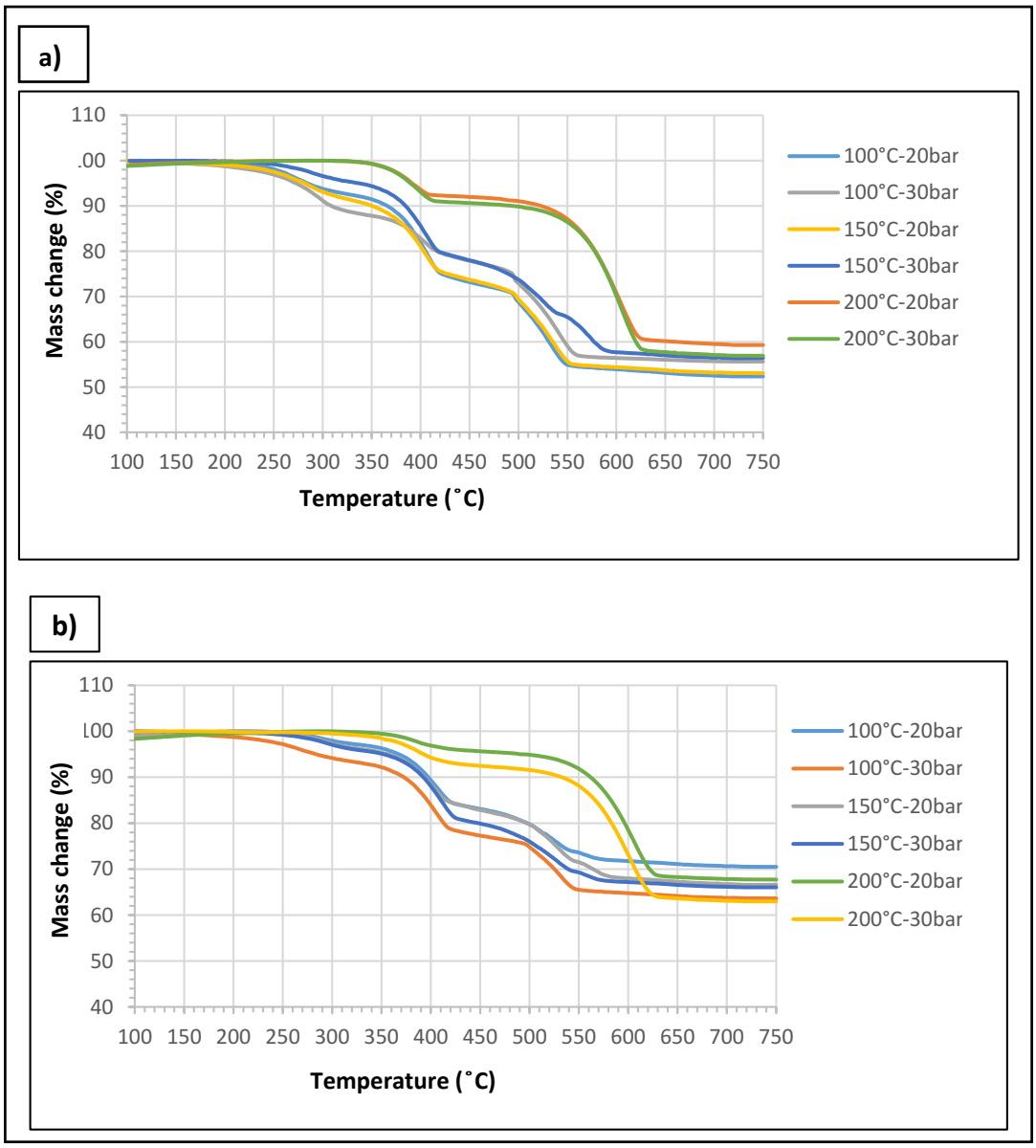

Fig 8. TGA thermal decomposition graph of precipitated phases, formed during aqueous carbonation of $Mg(OH)_2$ in heterogeneous carbonation using different seeding sites. a) Activated carbon and b) alumina.

Interestingly, the amount of magnesite concentration is the lowest with the alumina seeding, even lower than that for a seedless carbonation under 100 and 150˚C, despite that heterogeneous seeding nucleation sites should, at least, in theory, enhance the kinetics of nucleation.

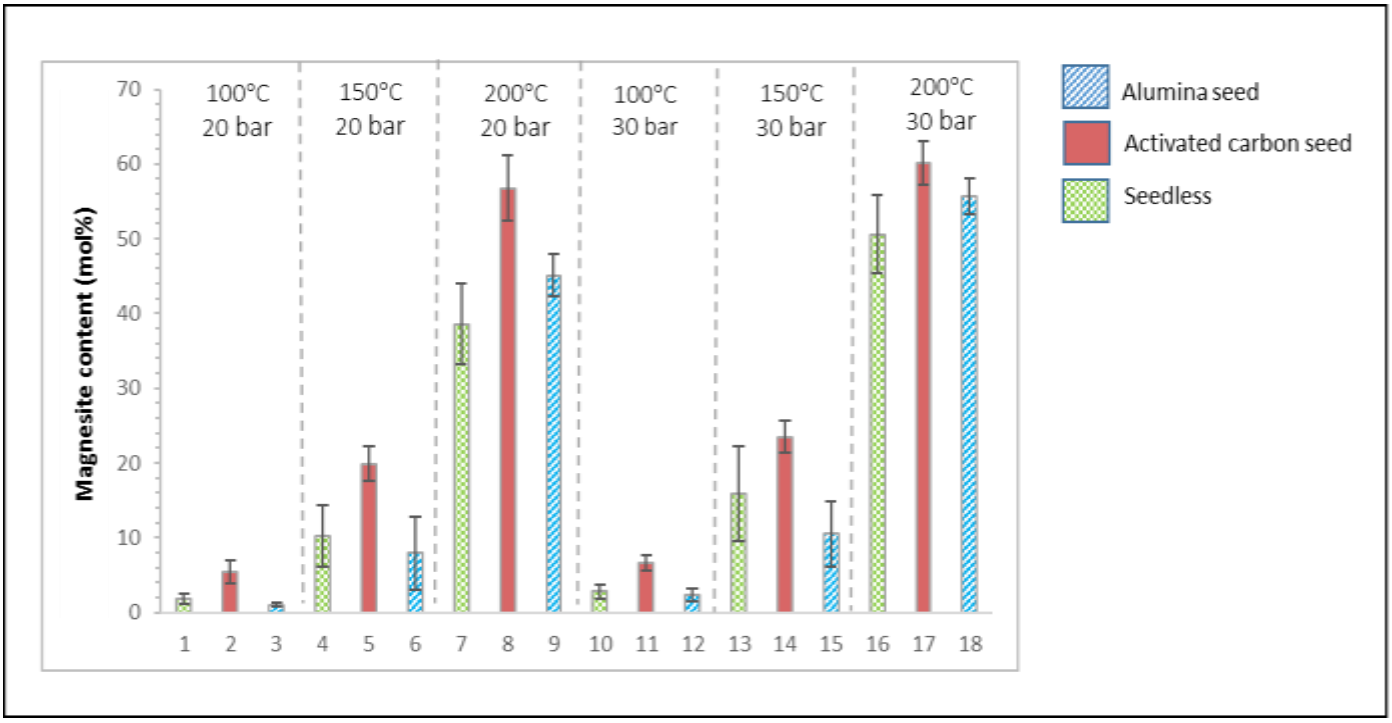

Fig 9. Magnesite molar concentration under varying carbonation temperature and pressure conditions, in precipitates formed during aqueous carbonation of $Mg(OH)_2$, under heterogeneous and seedless carbonation conditions.

This interesting finding can be explained considering the polar structure and hydrophilic property of alumina seeds which result in the hydrogen bond formation on the surface of alumina when it comes into contact with water [50-54]. This, in turn, impedes the liberation of water molecules during the transition of hydromagnesite into magnesite phase and totally reduces the rate of magnesite phase formation, causing a reduction of magnesite quantity during carbonation.

In contrast to the 100 and 150˚C cases, at the applied carbonation temperature of 200˚C and a pressure of 20 bar (Fig. 9), the concentration of magnesite phase is higher for the alumina seeding compared to the seedless carbonation, indicating clearly the dominant effect of high temperature and pressure on the hydromagnesite to magnesite transition through enhanced water liberation [24-29, 34, 45]. However, at 200°C and a high pressure of 30 bar the magnesite content (Fig. 9) reaches, within the experimental error,

nearly the same quantity for the alumina (bar # 18 in Fig. 9) and activated carbon (bar # 17 in Fig. 9) seeding. Apparently, the effects of high temperature and pressure overcome the transition barrier and the influence of heterogeneous seeding, either hydrophobic or hydrophilic, becomes less important although the activated carbon seeding still results in the highest magnesite content in Fig. 9 (bar # 17).

The total conversion percentage of the carbonation process was calculated based on the thermal method explained in section. (3.1). The results are presented in Fig. 10, and show a very similar trend to that of the magnesite molar percentage (Fig. 9). This result shows a primary effect of anhydrous phase formation on the total efficiency of the carbonation process as discussed earlier.

Quantitative assessment of the outcomes of this research shows that simultaneously controlling the applied temperature and pressure and the effective implementation of seeds can increase the efficiency of carbonation for a specific period of time. It is found that under the carbonation conditions of 200°C, CO_2 pressure of 30 bar and with activated carbon seeding, the molar percentage of favorable anhydrous magnesite phase in the carbonation products reaches about 60% (Fig. 9) with the corresponding carbonation conversion of about 72% (Fig. 10).

Furthermore, the proposed carbonation approach has shown a successful outcome, even under moderate temperature conditions of 100 and 150°C. The molar percentage of magnesite in Fig. 9 shows an increase of about 200% under the controlled conditions of 100°C and CO_2 pressure of 20 bar and about 23%, at 150°C and CO_2 pressure of 30 bar, using the activated carbon seeding, compared to similar conditions under seedless precipitation.

By comparison, in similar research on aqueous carbonation of $Mg(OH)_2$, Swanson et al. [24] reported the maximum magnesite concentration of about 98% which was achieved in one hour of carbonation at the carbonation temperature of 150°C and CO_2 pressure of 15 atm, through injecting magnesite sites in the solution. Their reported concentration is much larger than 60% obtained in this work (150°C, about 30 bar CO_2 and with activated carbon seeds) (Fig. 9). One reason for a larger concentration in [24] might be that their reactor was equipped with stirrer device which could facilitate the kinetics of mass transfer which was not employed in the present work. However, there is also a possibility that Swanson et al. [24] overestimated their results by not taking into account a separation issue between the quantity of the magnesite phase formed as an anhydrous precipitate during carbonation and the pre-injected magnesite seeds added to the solution intentionally, to form a preferred site of nucleation. The whole amount of mass change during decomposition of products in the decarbonation range of magnesite was attributed in [24] to the precipitated magnesite decomposition, neglecting whether the decomposed magnesite in that region was the product of carbonation or was a pre-injected seed. Furthermore, the portion of

magnesite formed during thermal analysis as a consequence of previously decomposed hydromagnesite (through sequenced dehydration (Eq. (5)) and dehydroxylation (Eq. (6)) was not differentiated from magnesite formed during carbonation. In other words, the overlap in thermal decomposition range between the third stage of hydromagnesite decomposition (Eq. (7)) and the magnesite decarbonation (Eq. (8)) has not been considered by Swanson et al. [24]. Hence, the whole TGA mass change during decarbonation was ascribed to precipitated anhydrous magnesite. Attributing the whole mass change reduction in the thermal range of decarbonation to magnesite as a carbonation product might have been the cause of noticeable differences between the results of this research and those reported in [24].

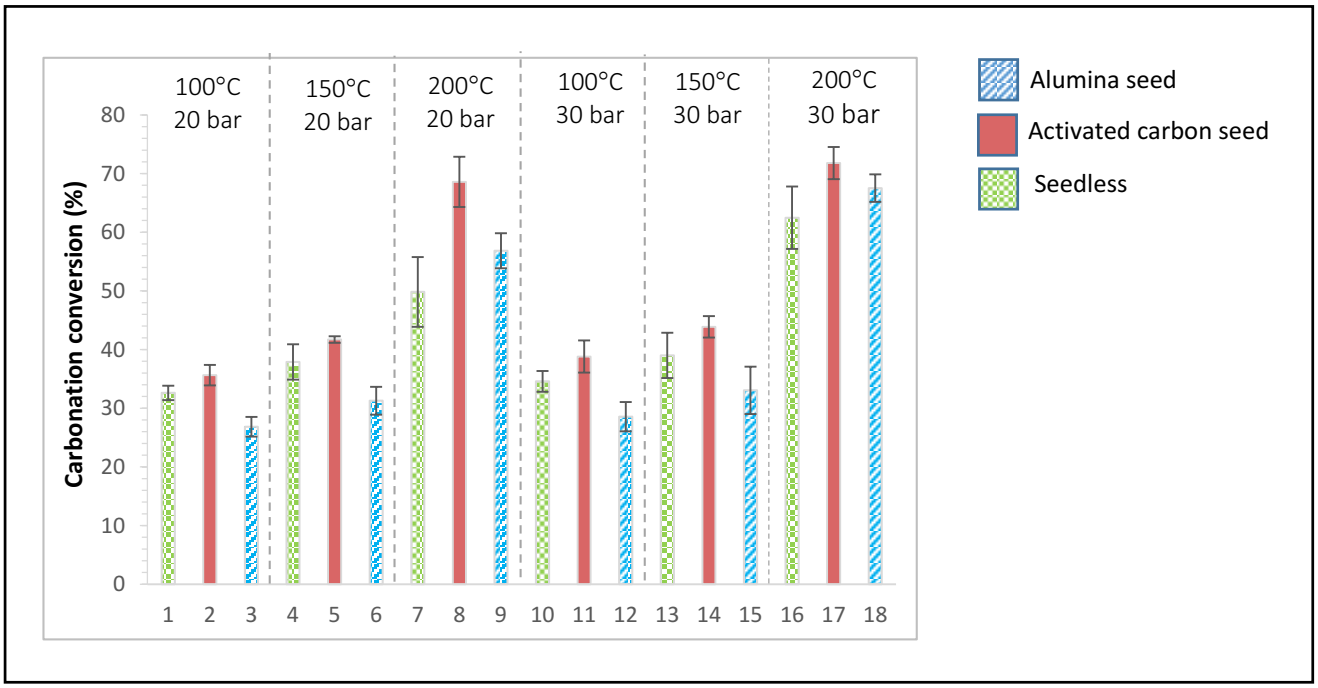

Fig 10. Carbonation conversion percentage under varied carbonation temperature and pressure conditions, in precipitates formed during aqueous carbonation of $Mg(OH)_2$, under heterogeneous and seedless carbonation conditions.

4. Future Work Suggestions

This study compares the efficiency of carbonation processes, under the implementation of two different seeding materials. The amount of SSA, as one of the most determinant parameters in mineral carbonation was designed to be kept constant and the hydrophobicity and surface properties were discussed in accordance to the previously offered mechanisms of precipitates' formation. However, still there might be other surface and structural differences between the implemented seeds, responsible for the different reported behaviors and performances. In this research the difference in behavior and

performance of implemented seeding materials was mostly attributed to wettability properties. Hence, comprehensive investigation of the other possible causes of difference such as surface charge, roughness and chemistry would be remained essential in order to come up with the most appropriate seeds, where the kinetics of precipitation is a limiting barrier.

The cost feasibility of mineral carbonation process has been assessed in several estimates. The total cost of wet direct carbonation of olivine is evaluated to be about \$69 / ton CO_2 in Albany Research Center, 2005 [55] at the temperature of 185°C and CO_2 pressure of 150 atm. The total cost of indirect mineral carbonation route using the compounds such as $Mg(OH)_2$ is even higher and is estimated to be in the range of 63€ (in 2001) and 30 € (in 1996) per ton of CO_2 for indirect $Mg(OH)_2$ carbonation using acetic acid and HCl extraction route, respectively [56-57]. In a comprehensive study, Giannoulakis et al. [58] evaluated the added cost of electricity generation in hard coal PC and NGCC power plants, in order to assess the economic performance of CCS process in fossil-fuel power generation chains. In this study the cost evaluation is performed for both direct mineral carbonation route, following National Energy Technology (NETL) approach on the Mg-silicate minerals [59-62], and indirect approach based on ÅAU (Åbo Akademi University) process [63-66] on $Mg(OH)_2$ [58]. According to their assessment, the total estimated added cost of direct aqueous carbonation process using Mg-silicate minerals is in the range of 135-170 and 84-94 € / ton CO_2 for hard coal PC and NGCC power plants, respectively. The added cost of indirect $Mg(OH)_2$ carbonation is estimated to be about 102-110 and 68-79 € / ton CO_2 for hard coal PC and NGCC power plants, respectively.

Finally, it needs to be mentioned that, although this research suggests effective strategies to enhance the efficiency of $Mg(OH)_2$ directed precipitation, the quantitative energy balance and economy efficiency analysis of the suggested carbonation process as an integral part of indirect mineral carbonation process, will still remain as a great motivation for future feasibility assessments [58]. Addressing the current assessed cost of mineral carbonation, the economic feasibility of CCS process still remains an issue and the study on the feasibility assessment and cost analysis of this process will remain a motivation for further future investigations. However, it needs to be emphasized that although the current study is not directly pointing to economic issues, it has an undeniable effect on the overall cost reduction of CCS process by developing a more efficient mineral carbonation process.

5. Conclusions

Directed precipitation of anhydrous magnesium carbonate ($MgCO_3$)/magnesite was investigated and evaluated in this work. Although the formation of magnesite is thermodynamically favorable, the slow rate of precipitation has been a limiting factor. Kinetics of precipitate nucleation and anhydrous magnesite formation (transition of hydromagnesite to magnesite) are enhanced through controlling the carbonation parameters and approaching heterogeneous carbonation. Controlling the carbonation temperature and pressure during seedless carbonation of $Mg(OH)_2$ was the initial approach to enhance the kinetics of magnesite formation. In addition, implementation of seeding (heterogeneous) nucleation sites, including alumina and activated carbon, has been suggested, in order to accelerate the kinetics of anhydrous magnesite precipitation. The research outcomes are summarized as follows. First, the effect of temperature and pressure on the variations of carbonation conversion (%) and magnesite content is examined. The similarity between the trends of carbonation conversion (%) and magnesite content as a function of temperature and pressure, points out towards the significant effect of the directed precipitation of anhydrous magnesite on enhancement of overall carbonation efficiency. Secondly, the role of preferred precipitation sites (heterogeneous seeding) on the directed precipitation of anhydrous magnesium carbonate and carbonation conversion percentage is significant. However, the influence of heterogeneous precipitation on directed precipitation is found to be dependent upon the nature of the precipitation sites. Finally, the effect of heterogeneous nucleation sites (seeding materials) on the directed precipitation of magnesite is related to the surface chemistry of seeds. Thus, hydrophobic activated carbon enhances the kinetics of directed precipitation more efficiently than hydrophilic alumina. This observation is explained by the mechanism of magnesite formation through the transition of initially formed hydromagnesite to magnesite and their dissimilar behavior in aqueous solution. A hydrophilic polar compound alumina, has a great tendency to form a hydrogen bond with water molecules in an aqueous solution which delays the liberation of water molecules as a critical stage of hydromagnesite to magnesite transition. In contrast, hydrophobic activated carbon accelerates the kinetics of hydromagnesite to magnesite transition as a result of its intrinsic water repelling effect. And thirdly, this approach shows that the simultaneous controlling of carbonation parameters accompanied by the implementation of heterogeneous sites succeeds in forming up to 60% magnesite molar concentration and a total conversion percentage of about 72%. Also, using activated carbon precipitation sites, even at the moderate thermal condition of 100 and 150°C, the magnesite molar concentration was increased by 200% and 23%, respectively, as compared to seedless condition. These findings are important for the future assessment of energy and economic performances of mineral carbonation for CO_2 capture and storage.

Acknowledgements

The authors thank Carbon Management Canada, the Natural Sciences and Engineering Research Council of Canada (NSERC) and Waterloo Institute for Nanotechnology for the research funding.

References

[1] Energy and climate change-World energy outlook-Special briefing for COP21 , International Energy Agency, France, 2015.

[2] Climate change: Review of greenhouse gases, in: Climate change, Emission, United States Environmental Protection Agency (EPA), USA, 2016. https://www3.epa.gov/climatechange/ghgemissions/gases.html

[3] T.A. Boden, G. Marland, R.J. Andres, Global fossil-Fuel CO_2 emissions, Carbon Dioxide Information Analysis Center, US Department of Energy (DOE), Oak Ridge national library, Tennessee, USA, 2010.

[4] Carbon dioxide: Projected emissions and concentrations, in, Intergovernmental Panel on Climate Change (IPCC), Department of Energy and Climate Change, 2014. http://www.ipcc-data.org/observ/ddc_co2.html

[5] Projections of future changes in climate-IPCC fourth assessment report, Climate change 2007: The physical science basis, 2007. https://www.ipcc.ch/publications_and_data/ar4/wg1/en/spmsspm-projections-of.html

[6] Trends in atmospheric carbon dioxide, in: Recent monthly average mauna Loa CO_2, US Department of Commerce-National Oceanic and Atmospheric Administration-Earth System Research Laboratory-Global Monitoring Division-NOAA Research, 2016. http://www.esrl.noaa.gov/gmd/ccgg/trends/

[7] K.J. Fricker, A.-H.A. Park, Effect of H_2O on $Mg(OH)_2$ carbonation pathways for combined CO_2 capture and storage, Chemical Engineering Science, 2013, 100, 332-341.

[8] M.J. McKelvy, A.V.G. Chizmeshya, J. Diefenbacher, H. Béarat, G. Wolf, Exploration of the role of heat activation in enhancing serpentine carbon sequestration reactions, Environmental Science & Technology, 2004, 38, 6897-6903.

[9] A.A. Olajire, A review of mineral carbonation technology in sequestration of CO_2, Journal of Petroleum Science and Engineering, 2013, 109, 364-392.

[10] S.R. Gislason, D. Wolff-Boenisch, A. Stefansson, E.H. Oelkers, E. Gunnlaugsson, H. Sigurdardottir, B. Sigfusson, W.S. Broecker, J.M. Matter, M. Stute, G. Axelsson, T. Fridriksson, Mineral sequestration of carbon dioxide in basalt: A pre-injection overview of the CarbFix project, International Journal of Greenhouse Gas Control, 2010, 4, 537-545.

[11] S.A. Bea, S.A. Wilson, K.U. Mayer, G.M. Dipple, I.M. Power, P. Gamazo, Reactive Transport modeling of natural carbon sequestration in ultramafic mine tailings, Vadose Zone Journal, 2012, 11, DOI:20110089.

[12] M. Aresta, Carbon dioxide as chemical feedstock, Wiley-VCH Verlag GmbH & Co. KGaA, Weinheim, Germany, 2010.

[13] R. Zevenhoven, S. Teir, Long-term storage of CO_2 as magnesium carbonate in Finland, in: 3rd annual conference on carbon capture and sequestration, Alexandria, 2004.

[14] R. Zevenhoven, S. Teir, S. Eloneva, Heat optimisation of a staged gas–solid mineral carbonation process for long-term CO_2 storage, Energy, 2008, 33, 362-370.

[15] S. Atashin, J.Z. Wen, R.A. Varin, Investigation of milling energy input on structural variations of processed olivine powders for CO_2 sequestration, Journal of Alloys and Compounds, 2015, 618, 555-561.

[16] T.A. Haug, Dissolution and carbonation of mechanically activated olivine- Investigating CO_2 sequestration possibilities, in: Faculty of Engineering Science and Technology, Department of Geology and Mineral Resources Engineering, NTNU-Trykk, Norwegian University of Science and Technology, Trondheim, Norway, 2010.

[17] D.C. Carnevale, Carbon sequestration potential of the coast range ophliolite in california, in: Environmental and Earth Sciences, University of Rhodeisland, USA, 2013.

[18] R.J. Rollason, J.M.C. Plane, A kinetic study of the reactions of MgO with H_2O, CO_2 and O_2: Implications for magnesium chemistry in the mesosphere, Physical Chemistry Chemical Physics, 2001, 3, 4733-4740.

[19] S. Atashin, J.Z. Wen, R.A. Varin, Optimizing milling energy for enhancement of solid-state magnesium sulfate ($MgSO_4$) thermal extraction for permanent CO_2 storage, RSC Advances, 2016, 6, 68860 - 68869.

[20] D.J. Fauth, P. Goldberg, J.P. Knoer, Y. Soong, W.K. O'Connor, D.C. Dahlin, D.N. Nilson, R.P. Walters, Carbon dioxide storage as mineral carbonates, Deviation of Fuel Chemical, American Chemical Society, 2000, 45 (4), 708-712.

[21] B. Garcia, V. Beaumont, E. Perfetti, V. Rouchon, D. Blanchet, P. Oger, G. Dromart, A.Y. Huc, F. Haeseler, Experiments and geochemical modelling of CO_2 sequestration by olivine: Potential, quantification, Applied Geochemistry, 2010, 25, 1383-1396.

[22] W.J.J. Huijgen, R.N.J. Comans, Carbon dioxide sequestration by mineral carbonation, Literature review, ECN-Clean Fossil Fuels Environmental Risk Assessment, ECN-C--03-016, (2003).

[23] S.A. Rockley, Carbon capture and storage, Elsevier, UK, 2010.

[24] E. Swanson, K. Fricker, M. Sun, A. Park, Directed precipitation of hydrated and anhydrous magnesium carbonates for carbon storage, Physical Chemistry Chemical Physics, 2014, 16, 23440-23450.

[25] G. Montes-Hernandez, F. Renarda, R. Chiriac, N. Findling, F. Toche, Rapid precipitation of magnesite micro-crystals from $Mg(OH)_2$-H_2O-CO_2 slurry enhanced by NaOH and a heat-ageing step (from 20 to 90°C), Crystal Growth & Design, 2012, 12, 5233–5240.

[26] mineral saturation index." A Dictionary of Earth Sciences". Retrieved November 11, 2016 from Encyclopedia.com: http://www.encyclopedia.com/science/dictionaries-thesauruses-pictures-and-press-releases/mineral-saturation-index

[27] M. Hänchen, V. Prigiobbe, R. Baciocchi, M. Mazzotti, Precipitation in the Mg-carbonate system—effects of temperature and CO_2 pressure, Chemical Engineering Science, 2008, 63, 1012–1028.

[28] H.T. Schaef, C.F. Windisch Jr., B.P. McGrail, P.F. Martin, K.M. Rosso, Brucite [$Mg(OH_2)$] carbonation in wet supercritical CO_2: An in situ high pressure X-ray diffraction study, Geochimica et Cosmochimica Acta, 2011, 75, 7458–7471.

[29] A.L. Harrison, I.M. Power, G.M. Dipple, Accelerated carbonation of brucite in mine tailings for carbon sequestration, Environmental Science & Technology, 2013, 47, 126−134.

[30] Y. Xiong , A.S. Lord, Experimental investigations of the reaction path in the MgO–CO_2 –H_2O system in solutions with various ionic strengths, and their applications to nuclear waste isolation, Applied Geochemistry, 2008, 23, 1634–1659.

[31] P.J. Davies, B. Bubela, The transaction of nesquehonite into hydromagnesite, Chemical Geology, 1973, 12, 289-300.

[32] L. Zhao, L. Sang, J. Chen, J. Ji, H.H. Teng, Aqueous carbonation of natural brucite: Relevance to CO_2 Sequestration, Environmental Science & Technology, 2010, 77, 406–411.

[33] A. Botha, C.A. St rydom, Preparation of a magnesium hydroxy carbonate from magnesium hydroxide, Hydrometallurgy, 2001, 62, 175– 183.

[34] D. Sheila, P.R. Khangaonkar, Precipitation of magnesium carbonate, Hydrometallurgy, 1989, 22, 249-258.

[35] N.R. Chevalier, Do surface wetting properties affect calcium carbonate heterogeneous nucleation and adhesion?, The Journal of Physical Chemistry, 2014, 118, 17600−17607.

[36] M. Donnet, P. Bowen, N. Jongen, H. Hofmann Use of seeds to control precipitation of calcium carbonate and determination of seed nature, Langmuir, 2005, 21, 100-108.

[37] D.R. Gaskell, Introduction to the thermodynamics of materials, 5th ed., CRC Press, USA, 2008.

[38] M. Földvári, Handbook of thermogravimetric system of minerals and its use in geological practice, in: Occasional papers of the geological institute of Hungary, Geological Institute of Hungary, Hungary, 2011.

[39] L.A. Hollingbery, T.R. Hull, Brucite ($Mg(OH)_2$), hudromagnesite ($Mg_5(CO_3)_4(OH)_2{\cdot}4H_2O$) and magnesite ($Mg(CO_3)$), Thermochimica Acta, 2010, 509, 1-11.

[40] C. Padeste, O. H.R, A. Relier, The thermal behaviour of pure and nickel-doped hydromagnesite in different atmosphers, Materials Research Bulletin, 1991, 26, 1263-1268.

[41] D.N. Todor, Thermal analysis of minerals, Abacus Press, England, 1976.

[42] Y. Sawada, K. Uematsu, N. Mizutani, M. Kato, Thermal decomposition of hydromagnesite $4MgCO_3{\cdot}Mg(OH)_2{\cdot}4H_2O$, Journal of Inorganic and Nuclear Chemistry, 1978, 40, 979-982.

[43] Y. Sawada, J. Yamaguchi, O. Sakurai, K. Uematsu, N. Mizutani, M. Kato, Thermogravimetric study on decomposition of hydromagnesite $4MgCO_3.Mg(OH)_2.4H_2O$, Thermochimica Acta, 1979, 32, 127-140.

[44] Y. Sawada, J. Yamaguchi, O. Sakurai, K. Uematsu, N. Mizutani, M. Kato, Isothermal differential scanning calorimetry on an exothermic phenomenon during thermal decomposition of hydromagnesite 4 $MgCO_3 \cdot Mg(OH)_2 \cdot 4\ H_2O$, Thermochimica Acta, 1979, 34, 233-237.

[45] P. Chu Zhang, H.L. Anderson, J.W. Kelly, J.L. Krumhansl, H.W. Papenguth, Kinetics and mechanisms of formation of magnesite from hydromagnesite in brine, Technical report SAN099-19456, Sandia National Laboratories, New Mexico, USA, 2000.

[46] G. Gadikota, E.J. Swanson, H. Zhao, A.-H.A. Park, Experimental design and data analysis for accurate estimation of reaction kinetics and conversion for carbon mineralization, Industrial & Engineering Chemistry Research, 2014, 53, 6664-6676.

[47] D.A. Porter, K. Easterling, M.Y. Sherif, Phase transformations in metals and alloys, 3rd ed., CRC Press, USA, 2009.

[48] T.F. Tadros, J.B. Rosenholm, Colloid stability: The role of surface forces, Wiley, USA, 2011.

[49] C. Tanford, Interfacial free energy and the hydrophobic effect in: Proceeding of National Academy of Science of United States, 76 (9), pp. 4175-4176 , USA, 1979.

[50] G. Lefe`vre, M. Duc, P. Lepeut, R. Caplain, M. Fe´doroff, Hydration of γ-alumina in water and its effects on surface reactivity, Langmuir, 2002, 18, 7530-7537.

[51] G. Azimi, R. Dhiman, H.M. Kwon, A.T. Paxson, K.K. Varanasi, Hydrophobicity of rare-earth oxide ceramics, Nature Materials, 2013, 12, 315–320.

[52] H. KC, W.F. Schneider, A. Curioni, W. Andreoni, The chemistry of water on alumina surfaces: reaction dynamics from first principles, Science, 1998, 282, 265-268.

[53] M. Akao, F. Marumo, S. Iwai, The crystal structure of hydromagnesite, Acta Crystallographica, 1974. B30, 2670-2672.

[54] M. Akao, S. Iwai, The hydrogen bonding of hydromagnesite, Acta Crystallographica, 1977, B33, 1273-1275.

[55] W.K. O'Connor, D.C. Dahlin, G.E. Rush, S.J. Gerdemann, L.R. Penner, and D.N. Nilsen, Aqueous mineral carbonation: Mineral availability, pretreatment, reaction parametrics and process studies, Office of Process Development, National Energy Technology Laboratory (formerly Albany Research Center), Office of Fossil Energy, US DOE,USA, 2005.

[56] M.Kakizawa, Yamasaki A, Y.AYanagisawa, new CO_2 disposal process using artificial rock weathering of calcium silicate accelerated by acetic acid, Energy, 2001, 26, 341–354.

[57] K.S. Lackner, D.P.Butt, C.H.Wendt, D.H.Sharp, Carbon dioxide disposal in solid form, Proceedings 21st international conference on coal utilization and fuel systems, Clearwater, Florida, 1996.

[58] S.Giannoulakis, K.Volkart, C. Bauer, Life cycle and cost assessment of mineral carbonation for carbon capture and storage in European power generation, International Journal of Greenhouse Gas Control, 21, 2014, 140–157.

[59] Gerdemann, S.J., D.C. Dahlin, W.K. O'Connor, L.R. Penner, Carbon dioxide sequestration by aqueous mneral carbonation of magnesium silicate minerals, 2nd Annual Conference on Carbon Sequestration, Alexandria, Virginia, 2003.

[60] O'Connor, W.K., D.C. Dahlin, D.N. Nilson, G.E. Rush, R.P. Walters, P.C. Turner, CO_2 storage in solid form: A study of direct mineral carbonation, 5th International Conference on Greenhouse GasTechnologies, Cairns, Australia, 2000.

[61] W.J.J. Huijgen, R.N.J. Comans, G.J. Witkamp, Cost evaluation of CO_2 sequestration by aqueous mineral carbonation, Energy Conversion and Management, 48, 2007, 1923-1935.

[62] W.J. J. Huijgen, G.J. Ruijg, R.N.J. Comans, G.J. Witkamp, Energy consumption and net CO_2 sequestration of aqueous mineral carbonation, Industrial & Engineering Chemistry Research, 45, 2006, 9184-9194.

[63] Nduagu, E., T. Bjorklof, J. Fugerlund, E. Makila, J. Salonen, H. Geerlings, R. Zevenhoven, Production of magnesium hydroxide from magnesium silicate for the purpose of CO_2 mineralization-part 2: Mg extraction modeling and application to different Mg silicate rocks, Minerals Engineering, 30, 2012, 87-94.

[64] Nduagu, E., J. Bergerson, R. Zevenhoven, Life cycle assessment of CO_2 sequestration in magnesium silicate rock-a comparative study, Energy conversion and manageent, 55 (2012) 116-126.

[65] Nduagu, E., I. Romao, J. Fugerlund, R. Zevenhoven, Performance assessment of producing $Mg(OH)_2$ for CO_2 mineral sequestration, Applied Energy, 106, 2013,116-126.

[66] Nduagu, E.I., J. Highfield, J. Chen, R. Zevenhoven, Mechanisms of serpentine - amonium sulfate reactions: Toward higher efficiencies in flux recovery and Mg extraction for CO_2 mineral sequestration, RSC Advances, 4, 2014, 64494-64505.